Chemical Science & Engineering Research

Ariviyal Publishing

Research Article

DOI: 10.36686/Ariviyal.CSER.2023.05.12.073

Chem. Sci. Eng. Res., 2023, 5(12), 35-42.

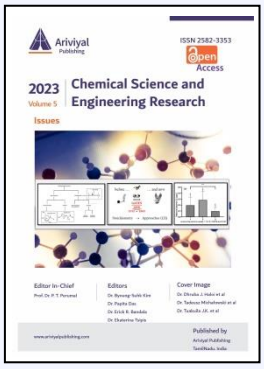

About the Role of a Human SPSI Homolog in the Living Cell (Alignments of B-Chain of Selenophosphate Synthetase (SPS) from *E. coli* Strain K12 (3U0O) and B-Chain of Human SPSI with Active Conformation (3FD6) and with AMP-CP as a Ligand (3FD5))

Yuliya V. Preobrazhenskaya* and Dmitry V. Preabrazhenski

Y.Kupala State University of Grodno, Grodno, Belarus 230001.

***Corresponding author E-mail address**: Yuliya.Preabrazh@gmail.com (Yuliya V. Preobrazhenskaya)

ISSN: 2582-3353

Crossref

Publication details
Received: 31st December 2022
Revised: 10th April 2023
Accepted: 10th April 2023
Published: 30th April 2023

Abstract: B-chains of the native selenophosphate synthetase (SPS) from strain K12 of *E. coli* (3U0OB) and of human SPS I (hSPSIB) was aligned with Swiss-Pdb Viewer and 24.8% identity was obtained with root mean square deviation (RMSD) of 1.48 Å. When aligned with Clustal Omega v.1.2.1, 3U0O B-chain truncated from the N-terminus till the 14th AA with B-chain of 3FD6 truncated from the N-terminus till the 13th AA, identity of 24.866% has been obtained for 93 AA. When hSPSIB and 3U0OB were aligned from the 1st AA residue with Clustal Omega v.1.2.1, 22.892% identity based on 95 AA was received using 3FD5 and 3FD6 as a reference. The aforementioned points out that the N-termini of hSPSI and the SPS from *E. coli* are variable. The structural alignment of the chain with the active conformation (3FD6B) and 3U0OB obtained with YASARA View shows the same 32.57% identity but lesser RMSD of 1.630 Å than the chain in inactive conformation (3FD5B), a RMSD of 1.669 Å over 218 aligned residues, under other equal parameters. It has been proposed to consider hSPSI as a Ser/Thr hydrolase.
The labelling experiments on Mn-ATP binding using the concentrations of the reagents 10-times lower then usually, 3.7 mkM WT or 3.4 mkM C17S E197D recombinant SPS and radioactive Mn-[8-^{14}C]ATP (0.5mM), have elucidated a right shoulder in the ATP-peak observed only with WT protein in the fractions eluted from the size-exclusive HPLC column. In the labelled protein peaks under enzyme turnover conditions, Mn-[8-^{14}C]-AMP was bound to the SPS in the amount of 10% from the total ^{14}C loaded.

Keywords: selenophosphate synthetase I-1; alignment-2; PDB-3; sequence identity-4; RMSD-5; active center-6; Ser/Thr hydrolase-7

1. Introduction

Selenophosphate synthetases (SPSases) (EC: 2.7.9.3) are wide-spread enzymes observed from archea to human, catalyzing a unique selenium donor formation from selenide and ATP:[1]

ATP + H_2O + hydrogenselenide = AMP + $2H^+$ + $phosphate_n$ + selenophosphate

Selenophosphate (SeP) is formed on the highly reactive Cys residue during a complicated chain of reactions starting from a nucleophylic attack on gamma-phosphate of ATP where putative nucleophile is still unknown.[2,3] It is clear that the sulfur atom of Cys forms a stable covalent S-Se bond. In Archea this is Cys-13,[3] in *E. coli* Cys-17 was found essential.[4] ATP and selenide are stoichiometrically converted to AMP and SeP in a 1:1 ratio and, supposing, 1 molecule of orthophosphate is formed. In the absence of selenide, though, a slow hydrolysis of ATP to AMP and orthophosphate could be preceded by SPS. At least one Walker motif consisting of Gly-X-Gly-XX-Gly was revealed in the structure of SPSases. It closely reminds the active center of ATP/GTPases. In mammalian genome two homologs of SPS were found: they normally were designated as SPSI and SPSII, from which only SPSII can exhibit selenide-dependent SPSase activity.[5-7] The role of SPSI in the organism remains indefinite.[8] There is only some information that the amount of mRNA transcript of SPSI in lung adenocarcinoma cells is higher by order.[9]

Currently, bioinformatic methods are widely used to study such macromolecules as proteins. In order to elucidate highly conservative regions in protein sequences between different classes of Biota a method of alignments has been applied lately. The aim of our investigation was to establish the location of an active center (centers) of SPS by means of linear and structural alignments of amino acid sequences of SPS subunits for representatives of different kingdoms of living beings – Bacteria and Animals.

2. Experimental Section

The "Swiss-PdbViewer" application v4.1.0 (https://spdbv.unil.ch/), Clustal Ω (Omega) v1.2.1, available on www.uniprot.org, and the

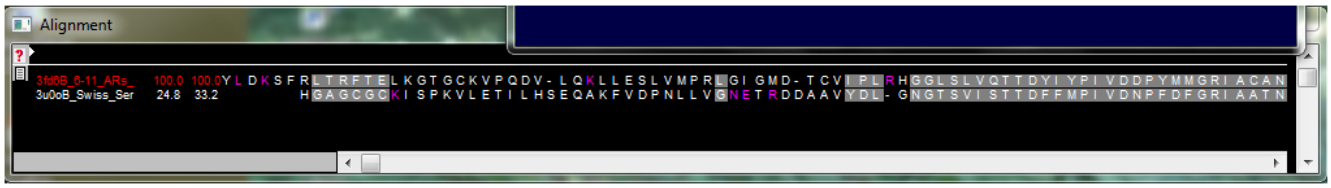

Fig. 1. Linear alignment of the 3U0O B-chain truncated from N-terminus till AA 13 with B-chain 3FD6 truncated from N-terminus till AA 12 when Iterative Magic Fit is applied with the "Backbone atoms only" option.

Fig. 2. Linear alignment of the 3U0O B-chain truncated from the N-terminus till AA 14 with the B-chain of 3FD6 truncated from the N-terminus till AA 13 when Iterative Magic Fit is applied with the "CA (carbon alpha) only" option.

"YASARA View" application (www.yasara.org/viewdl.htm) were used in our investigation. For UniProt (the Universal Protein Resource, www.uniprot.org), where Clustal Omega is built-in as a tool, the FASTA format of protein sequences has been used. PDB files have been retrieved from the PDB (Protein Data Bank) database for both Swiss-PdbViewer and YASARA View by entering corresponding PDB accession codes.

B-chain of native SPS from *E. coli* (3U0OB) and B-chain of human SPSI (hSPSIB) in complex with ADP and P_i (3FD6B) were aligned. B-chain 3U0O (N-terminus is cut till HIS13), B-chain in inactive conformation with AMP-CP (3FD5B) has been manually adjusted with trimming by 6-12 ARs from the N-terminus (N-terminus starts from GLU13); the truncation was made by means of Swiss-PdbViewer (menu "Build" > "Remove Selected Residues…"), selecting AA residues in Control Panel.

B-chain of 3U0O (N-terminus is cut till HIS13), B-chain of 3FD6 has been manually adjusted with trimming by 12 ARs from the N-terminus (N-terminus starts from LEU14).

For linear alignment of protein chain sequences we used the "Iterative Magic Fit" method (with the menu "Fit" > "Iterative Magic Fit" in Swiss-PdbViewer) optimized via minimization of the root mean square deviation (RMSD) between carbon alpha atoms (Fig. S1) as well as between backbone atoms (Fig. S2). In this method, hSPSI was used as a reference (fixed layer), that is the sequence of 3U0OB was being moved along the sequence of 3FD5B or 3FD6B.

Structural alignment of the corresponding amino acid sequences was made in "YASARA View" application with MUSTANG method.[10] The alignment has been executed via the menu "Analyze" > "Align" > "Pairwise, based on structure: Objects with MUSTANG". The sequences used were in the PDB format, inputted consequently as a "source" ("Hit" in terms of YASARA View) and a "target" ("Query" in terms of YASARA View).

2.1. Materials

[8-^{14}C]ATP (44.9mCi/mmol) was purchased from BioRad Laboratories.

2.2. Enzyme

Purification of a recombinant SPS E197D from *E.coli* BL21 transformed with a recombinant plasmid pET11aSelD containing a wild-type SelD gene was performed as described by us.[11]

2.3. Enzyme Activity

The ATPase activity of SPS in the absence of selenide was determined by the rate of AMP or ADP production. The reaction was conducted in 0.1M KOH-Tricine (pH 8.0) and 2mM $MnCl_2$ or $MgCl_2$, accordingly. After stopping the reaction by heating to 95˚C and separating the protein by centrifugation through 0.45 mkM Amicon filters, 50 mkM aliquotes were injected onto Apex C_{18} reverse-phase column (5 mkm).

2.4. Mn-ATP binding studies

Reaction mixtures (100 mkM aliquotes) containing 30 mkM SPS, 4 mM $MnCl_2$, 30 mM KCl, 2 mM [8-^{14}C]ATP (20 mkCi), 8-10 mM DTT in KOH-Tricine buffer 0.1M, pH 8.0 were incubated for 3 min and then were applied to a 0.7 × 60 cm TSK-gel SW2000 gel-filtration column. The column was pre-equilibrated with KOH-Tricine buffer 0.1M, pH 8.0, 0.5mM DTT and 4mM $MnCl_2$. The same buffer was used for the elution. The flow rate was 1ml/min and 1-ml-fractions were collected. The protein concentration was monitored at A_{280} and calculated using the extinction coefficient of 16,100 $(M \times cm)^{-1}$.[11] The radioactivity of each fraction was measured by liquid scintillation spectroscopy.

2.5. Ion-pair chromatography

To separate nucleotides after binding of Mn-ATP an HPLC ion-pair chromatography with the mobile phase as 0.1M TEA buffer (pH 8.0) was used. The distillation of the resulting nucleotides was performed on a C_{18} reverse-phase column (5 mkm) using a linear gradient of acetonitrile (0→5%). The nucleotides could be easily separated with that system for ion-pair chromatography, detected by UV-absorbancy measurements at 260 nm and very low concentrations of the product, AMP, could be detected. All the buffers and reagents were prepared from the highest grade chemicals available.

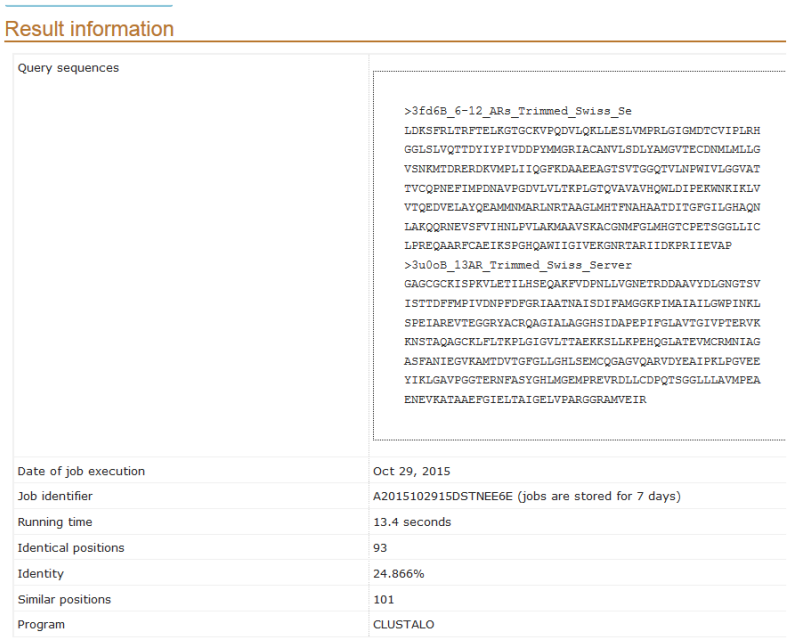

Result information

Query sequences	>3fd6B_6-12_ARs_Trimmed_Swiss_Se LDKSFRLTRFTELKGTGCKVPQDVLQKLLESLVMPRLGIGMDTCVIPLRH GGLSLVQTTDYIYPIVDDPYMMGRIACANVLSDLYAMGVTECDNMLMLLG VSNKMTDRERDKVMPLIIQGFKDAAEEAGTSVTGGQTVLNFWIVLGGVAT TVCQPNEPIMPDNAVPGDVLVLTKPLGTQVAVAVHQWLDIPEKWNKIKLV VTQEDVELAYQEAMMNMARLNRTAAGLMHTFNAHAATDITGFGILGHAQN LAKQQRNEVSFVIHNLPVLAKMAAVSKACGNMFGLMHGTCPETSGGLLIC LPREQAARFCAEIKSPGHQAWIIGIVEKGNRTARIIDKPRIIEVAP >3u0oB_13AR_Trimmed_Swiss_Server GAGCGCKISPKVLETILHSEQAKFVDPNLLVGNETRDDAAVYDLGNGTSV ISTTDFFMPIVDNPFDFGRIAATNAISDIFAMGGKPIMAIAILGWPINKL SPEIAREVTEGGRYACRQAGIALAGGHSIDAPEPIFGLAVTGIVPTERVK KNSTAQAGCKLFLTKPLGIGVLTTAEKKSLLKPEHQGLATEVMCRMNIAG ASFANIEGVKAMTDVTGFGLLGHLSEMCQGAGVQARVDYEAIPKLPGVEE YIKLGAVPGGTERNFASYGHLMGEMPREVRDLLCDPQTSGGLLLAVMPEA ENEVKATAAEFGIELTAIGELVPARGGRAMVEIR
Date of job execution	Oct 29, 2015
Job identifier	A2015102915DSTNEE6E (jobs are stored for 7 days)
Running time	13.4 seconds
Identical positions	93
Identity	24.866%
Similar positions	101
Program	CLUSTALO

Fig. 3. UniProt alignment between 3fd6B and 3u0oB result.

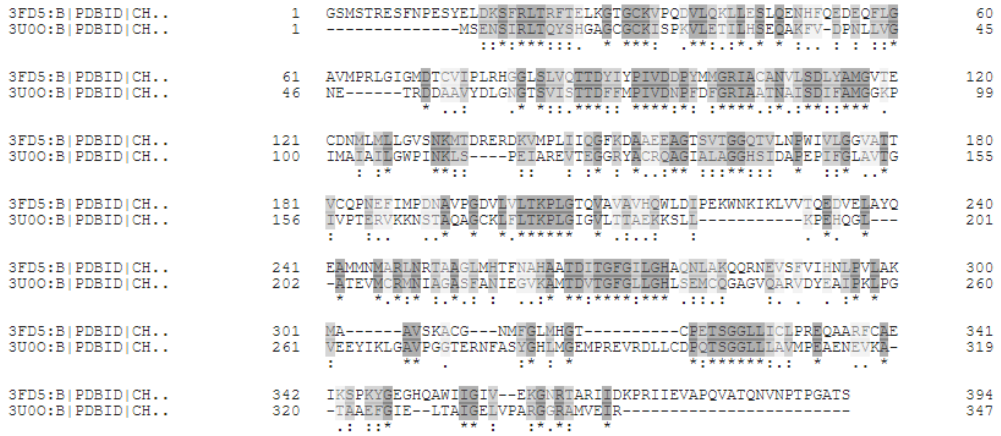

Fig. 4. Alignment of human SPSI 3FD5B and SPS from *E.coli* 3U0OB.

3. Results

Linear alignment of the 3U0O B-chain truncated from N-terminus till AA 13 with the B-chain of 3FD6 truncated from the N-terminus till AA 12 showed sequence-level 24.8% identity between them with RMSD = 1.48 Å with the "Iterative Magic Fit" method in case of the "Backbone atoms only" option was used (Fig. 1).

If the "CA (carbon alpha) only" option was used when applying Iterative Magic Fit, the linear alignment of the above B-chains of 3U0O and 3FD6 showed 24.5 percent identity with RMSD = 1.44 Å (Fig 2).

Linear alignment of the 3U0O B-chain with B-chain of 3FD5 both started from the 13th AA showed sequence-level identity 24.8% between them with RMSD = 1.48 Å using the "Iterative Magic Fit" method in case of the "Backbone atoms only" option was used. If the "CA (carbon alpha) only" option was used when applying Iterative Magic Fit, the alignment of the B-chains of the above proteins (3U0O and 3FD5) showed the same (24.8) percent identity with RMSD = 1.46 Å.

However, in case of Swiss-PdbViewer, the proteins were not fully aligned regarding the Gly-rich active center that is situated at the N-terminus.

When aligned 3U0O B-chain truncated from the N-terminus till AA 14 with B-chain of 3FD6 truncated from the N-terminus till AA 13, identity of 24.866% has been obtained with Clustal Omega v.1.2.1 publicly available on the UniProt web site www.uniprot.org (Fig. 3). The sequence alignment shows 93 identical positions.

When 3FD5 and 3U0O (B-chains) were aligned from the 1st AA residue with Clustal Omega v.1.2.1 on the UniProt web site, the sequence-level identity 22.892% based on 95 identical residues was received using 3FD5B as a reference (Fig. 4). Accordingly, when 3FD6 and 3U0O (B-chains) were aligned from the 1st AA residue with Clustal Omega v.1.2.1 on the UniProt web site, 22.892% identity based on 95 identical residues was received using 3FD6B as a reference. Similar percent identity for both conformations of SPSI is not surprising; however, UniProt does not allow determining RMSD, therefore, only a structural alignment with the YASARA View application provides suitable results that could shed the light to a

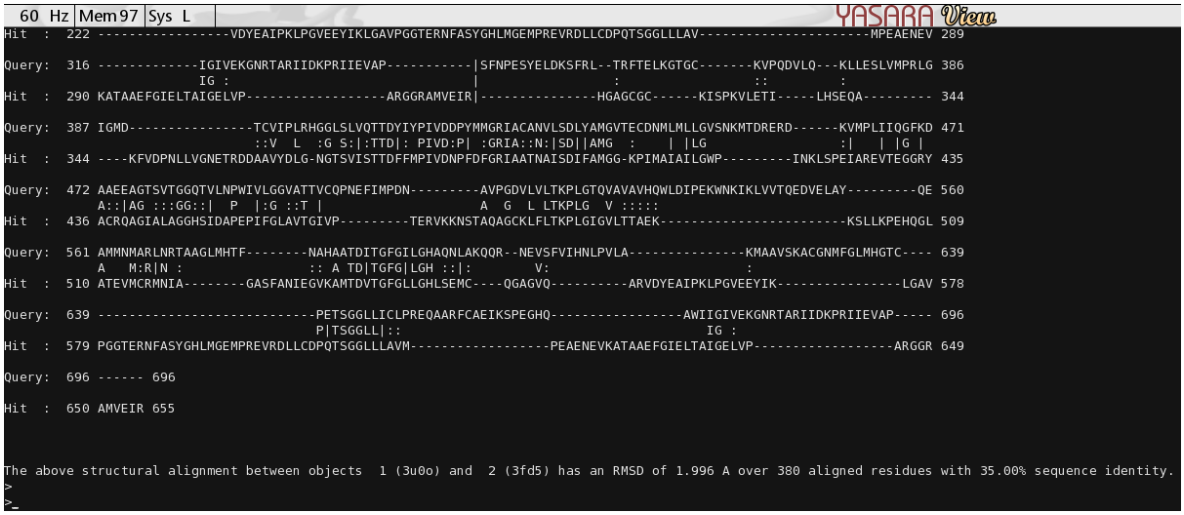

Fig. 5. Structural alignment between 3U0O as a source and 3FD5 as a target.

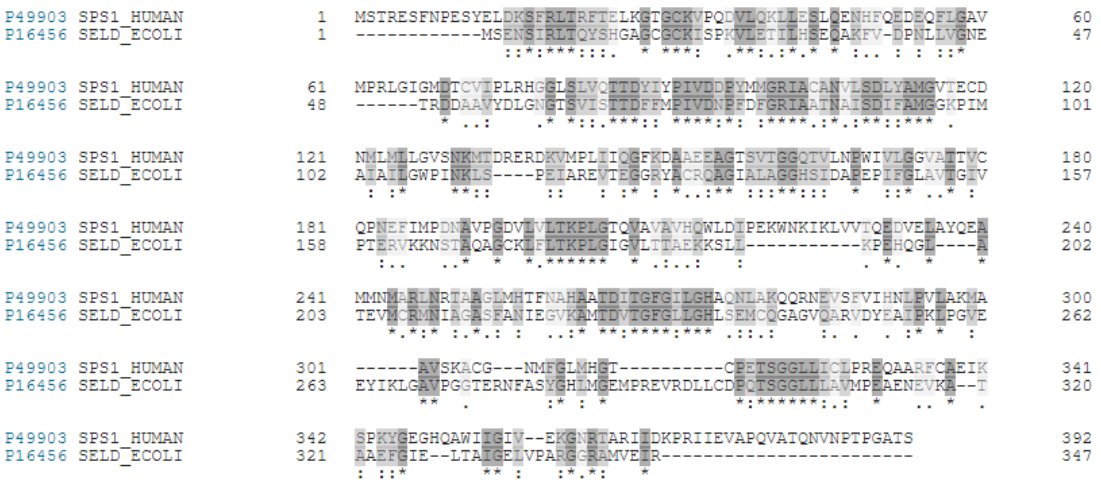

Fig. 6. Alignment of human SPSI and SPS from *E.coli* taken from the UniProt databases in FASTA format.

conformation of the protein. As it is stated above, alignment of 3U0O B-chain truncated from the N-terminus till AA 14 with the B-chain of 3FD6 truncated from the N-terminus till AA 13 showed identity of 24.866%. That means the N-terminus of hSPSI and of SPS from *E. coli* is variable. The N-terminal portion of selenophosphate synthetases has been shown to be highly flexible,[3,12,13,14] it depends on the presence of a ligand, and it is disordered in the crystal structure of the apo *A. aeolicus* SEPHS. [12]

When 3U0O was used as a source,[13] 3FD5 as a target, it showed 35.00 % identity with RMSD = 1.996 Å over 380 aligned residues (Fig. 5). When a source was 3FD5 and a target - 3U0O, we received 34.91% identity with RMSD = 2.002 Å over 381 aligned residues (Fig. S3). When 3U0O was used as a source, 3FD6 as a target, it showed 35.54% identity with RMSD = 1.983 Å over 377 aligned residues (Fig. S4). When a source was 3FD6 and a target - 3U0O, we also received 35.54% identity with RMSD = 1.983 Å over 377 aligned residues (Fig. S5). When *Trypanosoma leishmanii* SPS 5L16[11] was used as a source, 3FD6 as a target, it showed 47.74% identity with RMSD = 1.143 Å over 287 aligned residues.

We found that the structural alignment between 3U0OB and 3FD6B both started from the 13th AA residue obtained with YASARA View has shown an RMSD of 1.630 Å over 218 aligned residues with 32.57% identity (Fig. S6). The structural alignment between 3U0OB and 3FD5B both started from the 13th AA residue has shown an RMSD of 1.669 Å over 218 aligned residues with the same 32.57% identity (Fig. S7). These results indicate that the structural alignment of identical B-chains but with different ligands, under other equal parameters, results in equal percent identity but different RMSDs, at that, the chain with the active conformation (3FD6B) shows lesser RMSD.

When the sequences started from the 1st AA residue (Met) were aligned with Clustal Omega v.1.2.1 on the UniProt web site using the FASTA format, Cys17 of SPS from *E. coli* was aligned with Thr29 of human SPSI (Fig. 6).

Binding of ATP to the enzyme in the presence of Mg^{2+} is extremely low in the absence of selenide, but in the presence of Mn^{2+}, that does not support overall catalytic activity, binding of up to 0.8 eq. was observed. However, it was stated that in reaction mixtures containing Mn^{2+}, the high background levels of bound ATP interfered with direct detection of any phosphorylated intermediate that might have been formed in the partial reaction.[15] In our typical binding experiment the enzyme was separated at once from the

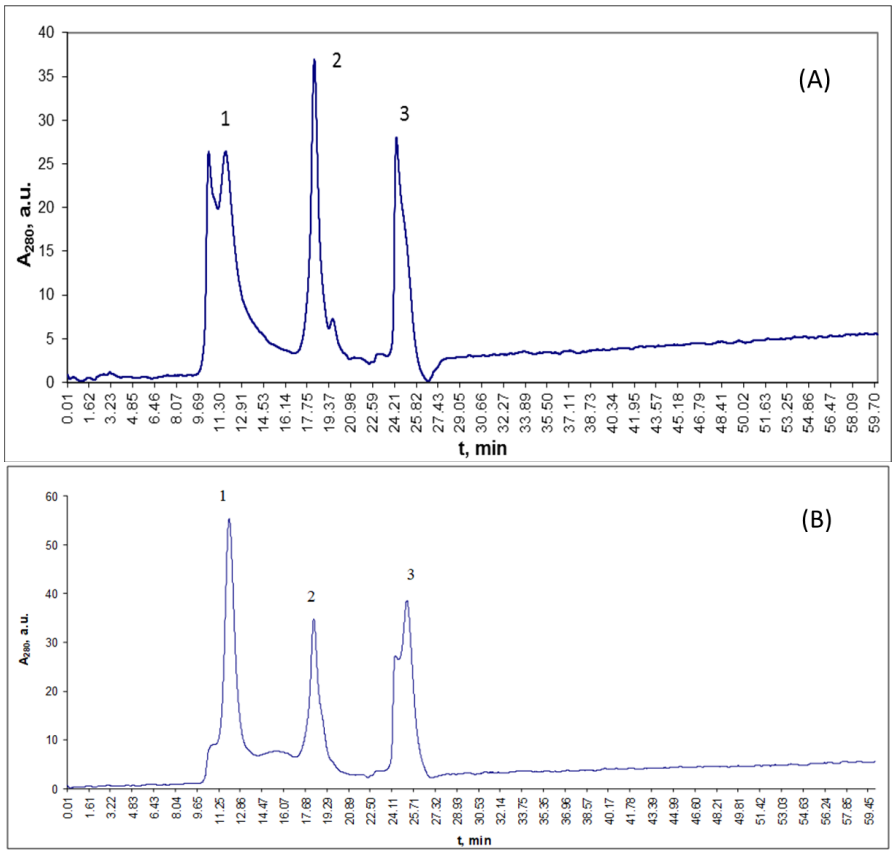

Fig. 7. Profiles of elution from size-exclusive HPLC column TSK 2000SW. A) wt recombinant protein [SPS E197D] = 3.7 mkM was mixed with the equimolar amount of ATP and loaded onto a size-exclusive HPLC column TSK 2000SW. The reaction buffer is 100 mM K-Tricine (pH 8.0), 30 mM KCl, 0.5 mM DTT, and 4 mM $MnCL_2$, as it is stated under Experimental. The same buffer was used to equilibrate the column. Peaks are designated as: 1. Protein; 2. ATP; 3 –DTT. B) The same as (A) but for C17S mutant.

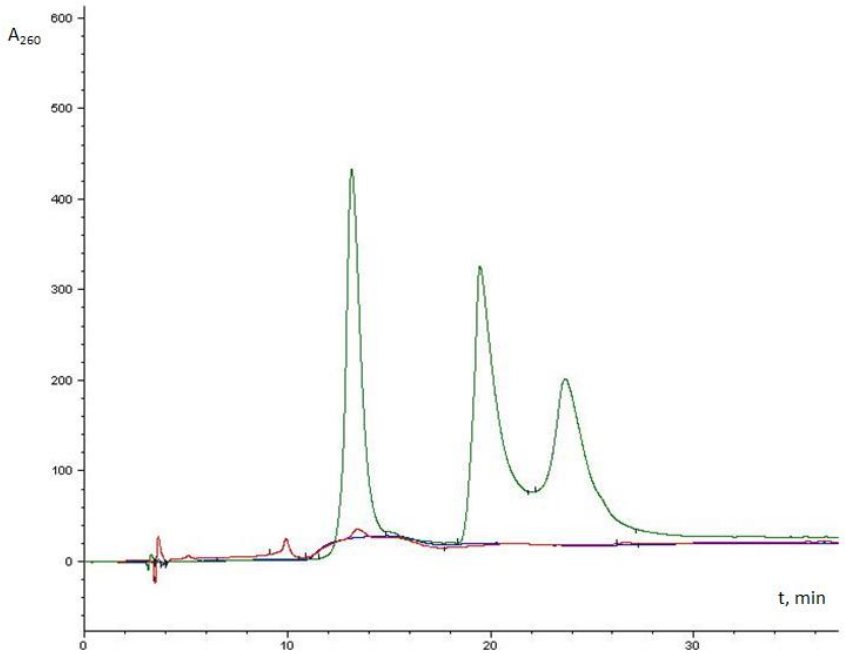

Fig. 8. HPLC identification of the enzyme-bound AMP formed during incubation with [8-^{14}C] ATP. A 100 mkl aliquot of the labelled enzyme peak eluted from the gel filtration column TSK-2000SW was applied to the C^{18} reverse phase HPLC column. The elution profile of standards of AMP, ADP and ATP (0.1mM of each) was overlayed onto the aliquot separation chromatogram and appears in green, whereas the aliquot profile – in red. The reaction mixtures used are given in the experimental section.

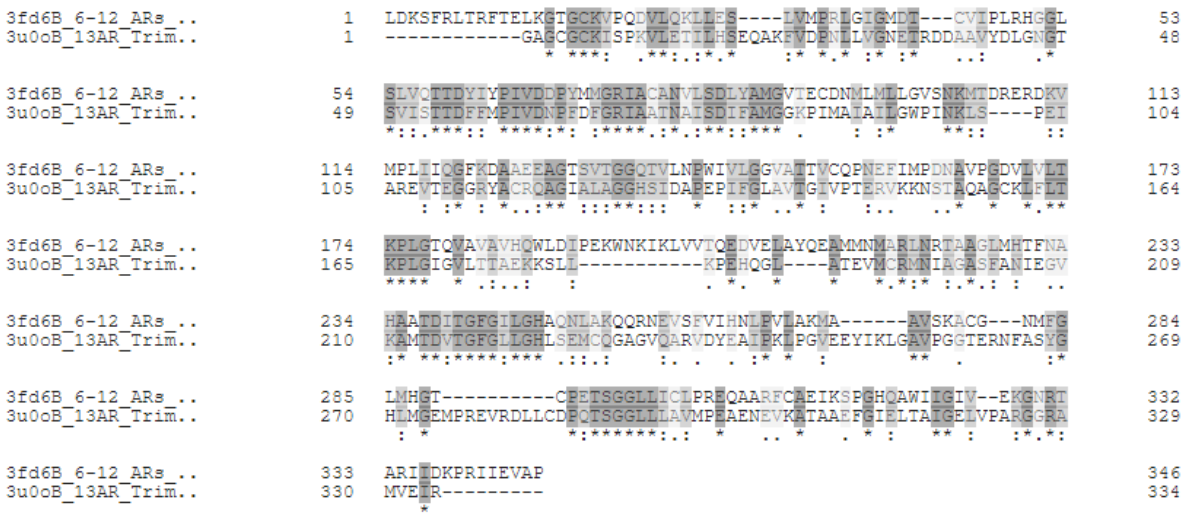

Fig. 9. Alignment of human SPSI 6-12AA trimmed -3FD6B and SPS from *E.coli* 3U0OB taken from the PDB databases in PDB format.

reagents by size-exclusive chromatography on a TSK-SW2000 column (7.5 mm × 60 cm) equilibrated and eluted with 100 mM KOH-Tricine, pH 8.0. Experiments were carried out with [8-^{14}C] ATP and 4mM $MnCl_2$ and the fractions containing both ^{14}C and the protein were termed "Mn-ATP bound". In order to avoid the high background levels of bound ATP we decreased the reaction concentrations of the protein and ATP till 10-fold as low. The results can be seen in the next chromatogram (Fig. 7). For the wt SPS E197D protein (A) the enzyme peak (1) remains 2-bumped and the second peak that was interpreted as an ATP-peak (2) has a right shoulder. In our experiment, about 10% of total ATP loaded onto the column was present in the form of ^{14}C-labeled enzyme peak and the rest 90% - in the form of free [8-^{14}C]-ATP. As far as [8-^{14}C]-ATP has a label in α-position, the right shoulder of ATP-peak that is not labelled, could not be ADP. However, it might be an intermediate of the reaction of Mn-ATP binding in the absence of selenide. In order to compare WT Mn-ATP binding with catalytically inactive mutant we performed the same experiment with C17S E197D and received no right shoulder in ATP-peak (2) Fig. 7 (B).

We picked up one aliquote of 100 mkl from the protein ^{14}C-labeled peak and loaded it onto a C^{18}–reverse-phase column to detect a ^{14}C-containing enzyme intermediate. Then we overlayed the chromatogram obtained onto the elution profile of standards of ATP, ADP and AMP, where the retention times were 13.6 min for AMP, 18.8 min for ADP, and 23.9 min for ATP. The result of that overlay could be seen in Fig. 8. It should be said that the assay for Mn-ATP binding was performed earlier but the content of the enzyme-labelled peak was not determined.[15] The calibration curve for AMP over 20-fold concentration range was linear, that allows to determine the amount of AMP formed quantitatively.

4. Discussion

The conserved Gly-rich region (Gly-X-Gly-X-X, 16-20 AA residues) remains aligned for the both proteins. This fact evidences that Cys is substituted with Thr in the human SPSI active center. This means human SPSI contains Thr in Gly-rich active center at the N-terminus that is constituent with Ser-Thr hydrolases. When we took PDB files from the protein database and aligned the sequences with Clustal Omega v.1.2.1 by means of Uniprot, we received the similar alignment with the same active center when trimmed 3FD5 by 6-12 AA (Fig. 9). We assume here that human SPSI belongs to the class of Ser/Thr hydrolases and could exhibit hydrolysis activity. Therefore, the role of the human homologous non-cysteine containing SPSI does not deal with Se metabolism, it deals with another class of enzymes that make hydrolysis in the living cell. It was established by us with bioinformatic methods, and it corresponds to the previous knowledge that the product of *SelD* gene is homologous to SPSII and, thereof, was named as SPSI. Suddenly it was found then, SPSI could not bind Se and did not exhibit SPSase activity.[8] All homologs named SPSI do not deal with selenophosphate synthesis.[8] After that, all the authors thought what the role of SPSI could be in the metabolism. We are the first who is proposing here to consider it as a Ser/Thr hydrolase. Lately some interesting papers about autoproteolysis have been published. In particular, it has been stated the substitution Ser→Thr decreases the activation energy of the reaction of autoproteolysis catalyzed with cis-autoproteolytic enzymes.[17] This determines threonine nucleophiles are evolutionary selected in autoproteolytic systems and, thereby, possibly SPSI is a product of SPSII autoproteolysis. About the change in nucleophyle such as Cys→Thr less is known, but these three nucleophiles as Ser→Cys→Thr are changeable between each other and some enzymes are familiar to use all three possible. In this content, the higher amount of mRNA transcript of SPSI in malignant cells by order is quite understandable that it is known the processes of autoproteolysis and larger amount of Ser/Thr hydrolases, other classes of hydrolases are found over there.[9] The authors declare the abundance of mRNA SPSI transcript in highly proliferating cells and, therefore, it only confirms our suggestion about the role of the enzyme in the living cell.[19]

The method that adjusts ends from the N-terminus during alignment has been automated by us and placed into the repositorium on GitHub. It could be seen here:

https://github.com/Dmitry150620/Trimming-Sequences/blob/Trimming-Sequences/Trimming_Sequences.txt or https://github.com/Yuliya-sudo/Sps-person/blob/6d8e773be085f5046b8f11555e3111bae0559d59/Trimming_Sequences.txt

It is the further study of the relationship between the function and the conformation of SPS as it was suggested earlier by us.[18] Again, our investigation indicates that crystallography studies of an inactivated protein could not always be useful in order to understand its reaction state as it was mentioned by the authors.[17]

As it was stated by the authors the amount of ^{75}Se (0.41 eq.) co-eluted with the enzyme peak was similar to that of ^{14}C-labeled AMP recovered in the separated enzyme fractions after incubation with [8-^{14}C]ATP under enzyme turnover conditions. It should be noted that the research was done with $MgCl_2$ not with $MnCl_2$ and it is said that it was fortuitous although it could be hardly understood what exactly is fortuitous: the equal amount of ^{75}Se and ^{14}C-labeled AMP or the presence of ^{14}C-labeled AMP in the labeled protein peak itself. Therefore, according to the results received and shown in Fig. 8 the amount of ^{14}C-labeled AMP is much smaller but it is Mn-ATP studies. It could be assumed that under these conditions the amount of ^{75}Se could be similar to that of ^{14}C-labeled AMP and that could mean that the formation of selenophosphate is not possible.[20] However, if to take into consideration that the reaction goes without selenide in the medium, and only ATP hydrolysis takes place it could mean that the back reaction of ATP formation goes faster under these conditions. It was shown that a specific monovalent cation-induced conformational state of the enzyme is observed when K^+ is present in the reaction medium and it is required for both: $MnCl_2$ binding and catalytic activity of the enzyme.[16] The authors state that it was [Mn-^{14}C] ATP bound, but there were no data that could essentially show that it is truly ATP stayed bound in the radioactive protein-bound peak fractions. It had been shown previously that AMP competitively inhibits SPSase activity. This data indicates the presence of a regulatory center in the SPS molecule that is distinct from the catalytic one. It had been confirmed with the data that the crystallization with AMP-CPP is possible only in open, that means, non-reactive state.[13]

5. Conclusions

B-chains of the native selenophosphate synthetase (SPS) from strain K12 of *E. coli* (3U0OB) and of human SPS I (hSPSIB) were aligned with Swiss-Pdb Viewer and 24.8% identity was obtained with root mean square deviation (RMSD) of 1.48 Å. When aligned with Clustal Omega v.1.2.1, 3U0O B-chain truncated from the N-terminus till the 14th amino acid (AA) with B-chain of 3FD6 truncated from the N-terminus till the 13th AA, identity of 24.866% has been obtained for 93 AA. When hSPSIB and 3U0OB were aligned from the 1st AA residue with Clustal Omega v.1.2.1, 22.892% identity based on 95 AA was received using 3FD5 and 3FD6 as a reference. The aforementioned points out that the N-termini of hSPSI and the SPS from *E. coli* are variable. The structural alignment of the chain with the active conformation (3FD6B) and 3U0OB obtained with YASARA View shows the same 32.57% identity but lesser RMSD of 1.630 Å than the chain in inactive conformation (3FD5B), a RMSD of 1.669 Å over 218 aligned residues, under other equal parameters. It has been proposed to consider hSPSI as a Ser/Thr hydrolase.

The labelling experiments on Mn-ATP binding using the concentrations of the reagents 10-times lower then usually, 3.7 mkM WT or 3.4 mkM C17S E197D recombinant SPS and radioactive Mn-[8-^{14}C] ATP (0.5 mM), have elucidated a right shoulder in the ATP-peak observed only with the WT protein in the fractions eluted from a size-exclusive HPLC column. In the labelled protein peaks under enzyme turnover conditions, Mn-[8-^{14}C]-AMP was bound to the SPS in the amount of 10% from the total ^{14}C loaded.

Supporting Information

Fig. S1 to Fig. S7 are given in the supporting file.

Conflicts of Interest

The authors declare no conflict of interest.

References

1 Yuan J.; Palioura S.; Salazar J.C.; Su D.; O'Donoghue P.; Hohn M.J.; Cardoso A.M.; Whitman W.B.; Söll D. RNA-Dependent Conversion of Phosphoserine Forms Selenocysteine in Eukaryotes and Archaea. *Proc. Natl. Acad. Sci.*, 2006, **103**, 18923-18927. [CrossRef]
2 Mullins L.S.; Hong S.B.; Gibson G.E.; Walker H.; Stadtman T.C.; Raushel F.M. Identification of a Phosphorylated Enzyme Intermediate in the Catalytic Mechanism for Selenophosphate Synthetase. *J. Am. Chem. Soc.*, 1997, **119**, 6684-6685. [CrossRef]
3 Itoh Y.; Sekine S.I.; Matsumoto E.; Akasaka R.; Takemoto C.; Shirouzu M.; Yokoyama S. Structure of Selenophosphate Synthetase Essential for Selenium Incorporation into Proteins and RNAs. *J. Mol. Biol.*, 2009, **385**, 1456-1469. [CrossRef]
4 Kim I.Y.; Veres Z.; Stadtman T.C. *Escherichia coli* Mutant SELD Enzymes. The Cysteine 17 Residue is Essential for Selenophosphate Formation from ATP and Selenide. *J. Biol. Chem.*, 1992, **267**, 19650-19654. [CrossRef]
5 Persson B.C.; Böck A.; Jäckle H.; Vorbrüggen G. SelD Homolog from Drosophila Lacking Selenide-Dependent Monoselenophosphate Synthetase Activity. *J. Mol. Biol.*, 1997, **274**, 174-180. [CrossRef]
6 Low S.C.; Harney J.W.; Berry M.J. Cloning and Functional Characterization of Human Selenophosphate Synthetase, an Essential Component of Selenoprotein Synthesis (∗). *J. Biol. Chem.*, 1995, **270**, 21659-21664. [CrossRef]
7 Xu X.M.; Carlson B.A.; Irons R.; Mix H.; Zhong N.; Gladyshev V.N.; Hatfield D.L. Selenophosphate Synthetase 2 is Essential for Selenoprotein Biosynthesis. *Biochem. J.*, 2007, **404**, 115-120. [CrossRef]
8 Mariotti M.; Santesmasses D.; Capella-Gutierrez S.; Mateo A.; Arnan C.; Johnson R.; D'Aniello S.; Yim S.H.; Gladyshev V.N.; Serras F.; Corominas M. Evolution of Selenophosphate Synthetases: Emergence and Relocation of Function Through Independent Duplications and Recurrent Subfunctionalization. *Genome Res.*, 2015, **25**, 1256-1267. [CrossRef]
9 Tamura T.; Yamamoto S.; Takahata M.; Sakaguchi H.; Tanaka H.; Stadtman T.C.; Inagaki K. Selenophosphate Synthetase Genes From Lung Adenocarcinoma Cells: Sps1 for Recycling L-Selenocysteine and Sps2 for Selenite Assimilation. *Proc. Natl. Acad. Sci.*, 2004, **101**, 16162-16167. [CrossRef]
10 Konagurthu A.S.; Whisstock J.C.; Stuckey P.J.; Lesk A.M. MUSTANG: A Multiple Structural Alignment Algorithm. *Proteins: Structure, Function, and Bioinformatics*, 2006, **64**, 559-574. [CrossRef]

11 Preobrazhenskaya Y.V.; Stenko A.I.; Shvarts M.V.; Lugovtsev V.Y. Binding Stoichiometry of a Recombinant Selenophosphate Synthetase with One Synonymic Substitution E197D to a Fluorescent Nucleotide Analog of ATP, TNP-ATP. *J. Amino Acids*, 2013, **2013,** 983565, 1-8. [CrossRef]
12 da Silva M.T.A.; Silva I.R.E.; Faim L.M.; Bellini N.K.; Pereira M.L.; Lima A.L.; de Jesus T.C.L.; Costa F.C.; Watanabe T.F.; Pereira H.D.M.; Valentini S.R. Trypanosomatid Selenophosphate Synthetase Structure, Function and Interaction with Selenocysteine lyase. *PLoS Negl. Trop. Dis.*, 2020, **14**, e0008091. [CrossRef]
13 Matsumoto E.; Sekine S.I.; Akasaka R.; Otta Y.; Katsura K.; Inoue M.; Kaminishi T.; Terada T.; Shirouzu M.; Yokoyama S. Structure of an N-terminally Truncated Selenophosphate Synthetase from Aquifex aeolicus. *Acta Crystallogr. Section F: Structural Biology and Crystallization Communications*, 2008, **64**, 453-458. [CrossRef]
14 Wang K.T.; Wang J.; Li L.F.; Su X.D. Crystal Structures of Catalytic Intermediates of Human Selenophosphate Synthetase 1. *J. Mol. Biol.*, 2009, **390**, 747-759. [CrossRef]
15 Noinaj N.; Wattanasak R.; Lee D.Y.; Wally J.L.; Piszczek G.; Chock P.B.; Stadtman T.C.; Buchanan S.K. Structural Insights into the Catalytic Mechanism of *Escherichia coli* Selenophosphate Synthetase. *J. Bacteriol.*, 2012, **194**, 499-508. [CrossRef]
16 Kim I.Y.; Stadtman T.C. Effects of Monovalent Cations and Divalent Metal Ions on *Escherichia coli* Selenophosphate Synthetase. *Proc. Natl. Acad. Sci.*, 1994, **91**, 7326-7329. [CrossRef]
17 Buller A.R.; Freeman M.F.; Wright N.T.; Schildbach J.F.; Townsend C.A. Insights into Cis-Autoproteolysis Reveal a Reactive State Formed Through Conformational Rearrangement. *Proc. Natl. Acad. Sci.*, 2012, **109**, 2308-2313. [CrossRef]
18 Preobrazhenskaya Y.V.; Sten'ko A.I.; Lugovtsev V.Y.; Moiseenok A.G.; Kuratchik O.M.; Mandrik K.A.; Voskoboev A.I. The Stoichiometry of Binding of ATP and Its Derivatives to a Recombinant Selenophosphate Synthetase E197D Catalytically Inactive Mutant C17S. *Adv. Biochem.*, 2017, **5**, 31-34. [CrossRef]
19 Na J.; Jung J.; Bang J.; Lu Q.; Carlson B.A.; Guo X.; Gladyshev V.N.; Kim J.; Hatfield D.L.; Lee B.J. Selenophosphate Synthetase 1 and its Role in Redox Homeostasis, Defense and Proliferation. *Free Radic. Biol. Med.*, 2018, **127**, 190-197. [CrossRef]
20 Liu S.Y.; Stadtman T.C. Selenophosphate Synthetase: Enzyme Labeling Studies with [γ-^{32}P] ATP,[β-^{32}P] ATP,[8-^{14}C] ATP, and [^{75}Se] Selenide. *Arch. Biochem. Biophys.*, 1997, **341**, 353-359. [CrossRef]